Geochemical Journal, Vol. 40, pp. 405 to 424, 2006

Strontium, $\delta^{18}O$ and $\delta^{13}C$ as palaeo-indicators of unconformities: Case of the Aleg and Abiod formations (Upper Cretaceous) in the Miskar Field, southeastern Tunisia

AMINA MABROUK,[1]* HABIB BELAYOUNI,[1] IAN JARVIS[2] and RICHARD T. J. MOODY[2]

[1]Département de Géologie, Faculté des Sciences de Tunis, Campus Universitaire 1060 Tunis, Tunisia
[2]School of Earth Sciences and Geography, Centre for Earth and Environmental Science Research, Kingston University, Penrhyn Road, Kingston upon Thames, Surrey KT1 2EE, U.K.

(*Received June 1, 2005; Accepted January 30, 2006*)

A carbon and oxygen stable-isotope study was undertaken on samples from the uppermost Turonian-Santonian Aleg Formation and the Campanian-lowest Maastrichtian Abiod Formation from four wells in the Miskar Field (W1, W2, W3, and W4), Gulf Gabès, offshore southeastern Tunisia. The strontium contents of the same samples were also determined. Carbon isotopes generally yielded values typical of Upper Cretaceous chalks. Calculation of palaeotemperatures using the $\delta^{18}O$ data obtained from the analysis of whole-rock samples from the four wells, in most cases generated higher values than those believed to characterize Santonian-Campanian ocean surface waters. This general negative shift in $\delta^{18}O$ values is thought to be related to alteration that has resulted from burial diagenesis. Strontium contents in the Abiod Formation are typical of Cretaceous - Tertiary chalks.

Top Aleg samples are depleted by around –0.6‰ $\delta^{18}O$ and –0.1‰ $\delta^{13}C$ compared to the Abiod samples, and by up to –300 μg/g Sr. Depletion in $\delta^{13}C$, $\delta^{18}O$ and strontium in the Aleg Formation is attributed to alteration by meteoric waters, indicating that the top of the Formation has been subject to both meteoric and burial diagenesis. This contrasts with the Abiod Formation which yields unaltered $\delta^{13}C$ and strontium values, and oxygen-isotope data which, although lighter than those typical of pristine Upper Cretaceous sediments, are heavier than those recorded in the Aleg Formation, suggesting that only burial diagenesis has affected the younger sediments. In our case, the use of the oxygen data for the calculation of marine palaeotemperatures is not reliable.

The strontium concentration, oxygen and carbon stable-isotope data indicate the presence of an unconformity between the Abiod Formation and the Aleg Formation, with possible subaerial exposure of the top of the Aleg Formation, probably during the Coniacian-Santonian and earliest Campanian. This result is consistent with the biostratigraphy of the four wells which confirms that an unconformity exists between the two formations.

Keywords: Tunisia, Cretaceous, chalk, strontium, carbon and oxygen stable-isotopes

INTRODUCTION

The strontium content of marine carbonates is controlled by the Sr/Ca ratio of seawater and by environmental, mineralogical and biological factors (vital effects) that control the partitioning of Sr (see Morse and Mackenzie, 1990 for a review). Subsequently, diagenetic effects may modify the primary signal, although in pelagic carbonates such effects are generally minimal. It is likely that typically 15–25% of the original Sr is lost to porewaters (Richter and Turekian, 1993; Stoll and Schrag, 2001), but such losses should uniformly affect individual stratigraphic profiles and should not significantly change stratigraphic trends. However, flushing by meteoric fluids may lead to significant Sr loss (e.g., Gross, 1964; Land and Epstein, 1970; Land 1979, 1986), and relatively low concentrations of Sr in calcites can also be produced in open-system marine diagenetic environments (Melim *et al*., 2002). Unaltered Cretaceous - Tertiary chalks typically contain around 1200 μg/g Sr (e.g., see Morse and Mackenzie, 1990). Strontium variation in pelagic sediments thus offers potential for stratigraphic, palaeoenvironmental and palaeoceanographic interpretation (cf., Renard, 1985, 1986; Stoll and Schrag, 2001), but such interpretations need to be made with caution and must be constrained by complementary petrographic and geochemical data.

Stable isotopic data from marine limestones and their constituent fossils and marine cements can provide quantitative evidence for changes in global climate and ocean circulation. Oxygen isotopic data can indicate changes in temperature and ocean composition, whereas stratigraphic

*Corresponding author (e-mail: aminamabrouk@yahoo.co.uk)

variation in carbon isotope ratio may reflect changes in the carbon cycle that can be linked to changes in oceanic productivity and atmospheric greenhouse gases (e.g., Marshall, 1981, 1992; Jenkyns *et al*., 1994; Huber *et al*., 1995; Abreu *et al*., 1998; Weissert *et al*., 1998; Clarke and Jenkyns, 1999; Saint-Germes *et al*., 2000; Jarvis *et al*., 2001, 2002). However, the precipitation of carbonates involves significant oxygen isotopic fractionation within a system assumed to be isotopically equilibrated: the composition of the precipitated mineral is related to the composition of the fluid from which it precipitated by a temperature-dependant fractionation factor.

The carbon isotopic composition of dissolved inorganic carbon (DIC) in seawater, on the other hand, is maintained close to zero through a balance of fluxes in the carbon cycle. This balance consists mainly of: (1) inputs through organic and inorganic carbon terrestrial sources and the oxidation of marine organic matter; (2) outputs through the production of marine carbonates and the production and burial of marine organic matter. Marine organic matter is usually withdrawn from the dissolved inorganic carbon in surface water, to be re-oxidized in deeper waters. As a consequence, the lighter carbon isotope is released and returns to the DIC. This difference in the isotopic composition between surface and deep waters reflects productivity and circulation within the oceans.

The carbon isotopic composition of calcium carbonate precipitated from aqueous solutions is controlled by various factors including: (1) the $\delta^{13}C$ of the CO_2 gas; (2) fractionation of carbon isotopes between CO_2 gas, carbonate and carbonate ions in solution; and the solid calcium carbonate; (3) the hydrogen ion activity (pH) of the solution; (4) and the temperature of isotopic equilibration. However, the equilibrium carbon isotopic fractionation effects between precipitating carbonate and surrounding bicarbonate are small and temperature effects are relatively minor. For instance, the relationships determined by Emrich *et al*. (1970) imply $\delta^{13}C$ enrichment in the solid of 1.85‰ at 25°C and the $\delta^{13}C_{calcite}$ increases by approximately 1‰ for every 27°C increase in temperature. Precipitated aragonite also has higher $\delta^{13}C$ than ambient dissolved inorganic carbon but the fractionation seems to decrease with increasing temperature (Grossman and Ku, 1986).

The relatively minor temperature dependency of the carbon isotope fractionation effects, and uncertainties over the magnitude of variation, negate the use of carbon isotopic values for temperature determination, but stratigraphic changes in carbonate carbon values are extremely useful as indicators of changes in the composition of the marine bicarbonate reservoir (Marshall, 1992). Conversely, oxygen isotopes can be used as palaeothermometers, in fact systematic differences in the $\delta^{18}O$ values of cogenetic minerals may be interpreted in terms of the temperature at which they equilibrated their oxygen with a common reservoir.

The oxygen isotope geochemistry of other calcium carbonate minerals differs from the behaviour of pure calcite. Magnesium calcite precipitated inorganically at 25°C is enriched in ^{18}O relative to pure calcite at the same temperature by 0.06‰ per mole % $MgCO_3$ (Tarutani *et al*., 1969). Grossman and Ku (1986) proposed that aragonite is enriched in ^{18}O with respect to calcite by 1.0‰ at 0°C to 0.5‰ at 20°C. Experimental studies at elevated temperatures suggest that dolomite formed at 25°C should be enriched in ^{18}O by 5‰ to 7‰ compared to coexisting calcite (Tan and Hudson, 1971). Matthews and Katz (1977) showed that the $\delta^{18}O$ of $CaCO_3$ increases continuously as Mg or Sr enter the $CaCO_3$ structure. However, in most natural samples, the difference in $\delta^{18}O$ values between coexisting calcite and dolomite is significantly less than predicted, which could be the result of three probable causes: (1) the isotope fractionation of dolomite relative to calcite is less than predicted; (2) dolomite is deposited as proto-dolomite which has a different fractionation factor, and is later transformed to dolomite with further fractionation; (3) dolomite originates from alteration of calcite and its ^{18}O isotopic composition depends on the $\delta^{18}O$ of the dolomitizing solution.

Despite the above significance of the two stable isotopes, the interpretation of data from geological samples can be hindered by the degree to which diagenesis has affected the primary oceanographic isotope signal (Hudson, 1977; Zachos *et al*., 1989). This was emphasized by Mitchell *et al*. (1997) who studied the stable-isotope composition of individual microfossils and cement samples from a Cenomanian-Turonian boundary chalk section at Dover, England. They proposed that the presence of mixing lines between primary compositions and cement make suspect simplistic palaeoceanographic and stratigraphic interpretations of sediments using stable isotopes. Conversely, several studies have demonstrated the usefulness of carbon and oxygen isotopes as palaeooceanographic, stratigraphic, and palaeoclimate indicators (e.g., Douglas and Savin, 1975; Scholle and Arthur, 1980; Pomerol, 1983; Jenkyns and Clayton, 1986; Schlanger *et al*., 1987; Parrish and Spicer, 1988; Spicer and Parrish, 1990, Spicer and Corfield, 1992; Gale *et al*., 1993; Paul *et al*., 1994; Accarie *et al*., 1996).

Jenkyns (1980) showed that a major positive $\delta^{13}C$ excursion present in the latest Cenomanian and earliest Turonian is a consistent stratigraphic marker that was associated with the widespread deposition of organic-rich shales on the shelves and in the ocean basins at that time. An increase in the rate of withdrawal of isotopically light carbon in the form of organic matter leaves the residual dissolved inorganic carbon (DIC) isotopically heavy.

Arthur *et al*. (1987) studying the Cenomanian/Turonian boundary carbon isotope event related the marked positive excursion to the deposition of black shale facies in the North Atlantic and to global oceanic anoxic events, and confirmed the presence of an isotope excursion in sediments deposited on continental margins and in epicontinental seas.

Schönfeld *et al*. (1991) determined the carbon and oxygen isotope composition of the Upper Cretaceous (Middle Coniacian to Lower Maastrichtian) white chalk of Lägerdorf-Kronsmoor, NW Germany. Their study focused especially on scrutinizing $\delta^{18}O$ compositions of the bulk rock, planktonic foraminifera, and inoceramids to evaluate diagenesis, specify the original environmental signals, and interpret palaeotemperature variation during the Middle Coniacian to Early Maastrichtian interval. Jenkyns *et al*. (1994) developed carbon- and oxygen-isotope stratigraphies for the Cenomanian-Campanian in southern England, the Campanian-Maastrichtian in eastern England, and the Upper Albian-Campanian in central Italy. The authors recorded several positive $\delta^{13}C$ excursions through the Cenomanian to basal Campanian (especially the positive excursion known to accompany the Cenomanian-Turonian boundary). Jenkyns *et al*. (1994) compared the $\delta^{18}O$ signals with previously published data in other parts of the world to suggest that the English Chalk records reflect a global signal of climatic change, and that the Cenomanian-Turonian boundary represents a turning point from a warming period to cooler climate.

Huber *et al*. (1995) using oxygen isotopes analyzed in planktonic foraminifera from the South Atlantic and the southern Indian oceans, confirmed a gradual warming of surface waters from the Albian through the Cenomanian followed by extremely warm surface waters from the Turonian through to the Early Campanian, and a long-term cooling of surface waters beginning in the late Early Campanian, continuing through to the end of the Maastrichtian.

Jenkyns *et al*. (1995) analysed carbon and oxygen isotopes of Cenomanian-Maastrichtian deep-water sediments from the north-central Pacific (ODP Site 869, flank of Pikinni-Wodjebato, Marshall Islands). Comparing these isotopic signals to others previously established in other parts of the world, the authors suggested that Cenomanian-Maastrichtian Pacific ocean-water had a similar isotopic chemistry to that of the Atlantic Ocean, the Tethyan Ocean, and European shelf seas.

Elorza *et al*. (1997) used oxygen isotope signals of inoceramid bivalves and belemnite rostra from three sections in the Liège and Limburg provinces (Belgium) to assess diagenesis and palaeotemperature evolution through the Late Campanian-Early Maastrichtian interval. Clarke and Jenkyns (1999) used new $\delta^{18}O$ results from chalk successions on the Exmouth Plateau of Western Australia, together with previously published data, to establish that the highest temperatures of the past 115 Myr (in excess of 33°C) occurred from the Cenomanian-Turonian boundary through to the Middle Turonian. In this work, the authors confirmed that the Cenomanian-Turonian boundary anoxic event was a major factor influencing climatic evolution, a conjecture previously made by Arthur *et al*. (1988) and Jenkyns *et al*. (1994). The new and reviewed $\delta^{18}O$ profiles of the Southern Hemisphere demonstrate short-term cooling and warming episodes during the Aptian-Maastrichtian, superimposed on two long-term warming and cooling periods that occurred during the Aptian-Turonian and Turonian-Maastrichtian respectively. The cooling period extended into the Eocene, as documented previously by Zachos *et al*. (1994).

Li *et al*. (2000) studied sea-level changes during the Campanian-Maastrichtian interval in NW Tunisia (El Kef and Elles sections). Their study focused on combining field work, macro- and micropalaeontological determinations, bulk-rock compositions, clay mineralogies, carbon and oxygen isotopes, total organic carbon (TOC), and Sr/Ca ratios to identify seven major sea-level cycles in the south-western Tethys during the last 10 Myr of the Cretaceous.

Jarvis *et al*. (2002) working on the Campanian-basal Maastrichtian pelagic-hemipelagic carbonates of Le Kef in Tunisia established a carbon-isotope stratigraphic correlation with south-western France (northern Tethys domain) and eastern England (Boreal domain). The authors indicated that major shifts in $\delta^{13}C$ profiles coincide with changes in eustatic sea-level, providing specific chronostratigraphic trends that may be used for bed-scale inter-continental correlation independent of biostratigraphy.

The success of previous studies on Upper Cretaceous stable-isotopic signatures prompted their use in the present study. The aim was to determine the stable isotopic compositions and strontium contents of the Abiod Formation and the uppermost Aleg Formation in southeastern Tunisia, in order to assess diagenesis and to try and establish notable stratigraphic event(s) within the Turonian-Lower Maastrichtian interval that might be recognized using isotopic and elemental geochemical criteria.

GEOLOGICAL BACKGROUND

Chalk deposition characterized most of the Late Cretaceous Epoch in many areas of the world. In Tunisia, it occurred predominantly during the Campanian-Maastrichtian ages (Fig. 1). The facies, characteristic of the Abiod Chalk Formation, shows high potential as a petroleum reservoir rock. In the offshore, the formation constitutes a major target for oil and gas exploration and

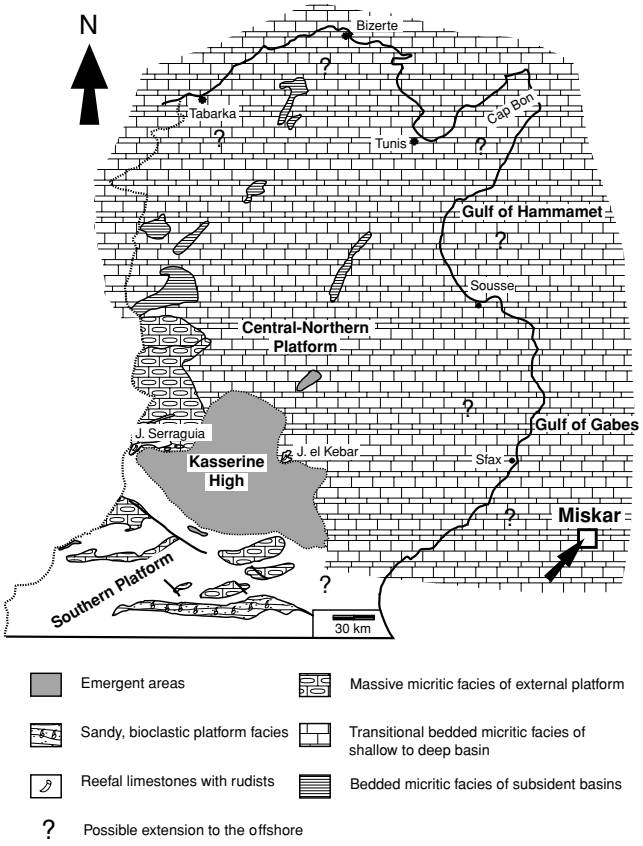

Fig. 1. Palaeogeographic map of Tunisia during the Campanian-Maastrichtian (modified from Negra (1994)).

exploitation and it has been cored in several wells, including those of the Miskar Field. The Field, part of the Amilcar permit (Fig. 2), is located in the Gulf of Gabès (southeastern Tunisia), 125 km offshore in 60 m of water.

The Miskar Field lies on the Pelagian Platform (Fig. 2), where an incipient rift system developed during the Early Cretaceous to Eocene. This rift system is expressed as a series of horsts and tilted fault blocks, including those found in the Miskar and Jugurtha fields. The Miskar structure (Fig. 3) is a broad N-S horst block affected by various faults generated throughout a complicated tectonic history (British Gas, 1990). The thickest Upper Cretaceous sequence exists to the north of the horst. Two major faults bound the structure to the west and the east, delimiting deep grabens, particularly to the east. Other faults exist in the central part, and break the horst into smaller fault blocks.

Based on seismic data, a thin Abiod Formation has been mapped on the horst, trending from Miskar well W1 in the north, to well W4 in the south (Fig. 3); thickness values are in the order of 50 m to over 80 m. The Abiod Formation thins to the east and northeast of the horst (40 to 50 m), where a high fault block occurs, from which the Formation has been completely eroded (Fig. 3). To the NW of the major western bounding fault, the formation thickens significantly to over 300 m.

The Miskar area was a structural high throughout the Cretaceous, enduring several phases of tectonic activity (British Gas, 1990). It is believed that the Miskar area was affected by five phases of movement from Cretaceous into the Cenozoic, which can be summarized as follows:

(i) the Zebbag Formation (Cenomanian-Turonian) was deposited on a pre-existing palaeo-high trending N-S with major faults bounding the structure to the east and west;

(ii) Zebbag to "Aleg carbonate marker" sediments (Cenomanian-lower Coniacian) seem to have been deposited during a relatively stable tectonic phase. Reactivation of old faults may have contributed to the irregular distribution of the lower Aleg;

(iii) during the deposition of the middle-upper Aleg (Coniacian-Santonian), normal faulting and intense deformation, especially towards the western flank of the structure took place. This activity combined with the pre-existing morphostructure of the basin induced thinning of sediments on the crest of the anticline, and the deposition of a considerable thickness of sediments on the flanks. The Campanian-Early Maastrichtian (Abiod Formation deposition) was characterized by a phase of relatively stable tectonic conditions;

(iv) tectonic activity increased again during the Paleocene with reactivation of normal faults, but a continued dominance of the main anticlinal structure;

(v) tectonic activity declined by the end of deposition of the Paleocene El Haria Formation which covers the whole structure. This was followed by a stable phase and the conformable deposition of clastic sediments. The structure is considered to have stabilized by the Late Eocene, and this is demonstrated by the Souar Formation which has a shallow regional dip to the southeast.

SAMPLING

Four cored wells form the basis of this study (Fig. 3). Cored intervals of the uppermost Aleg and the entire Abiod formations were logged and sampled in detail from four Miskar wells (W1, W2, W3, W4). All samples were selected for strontium analysis. However, only samples from the Miskar W1 and W4 wells, plus a few representative samples from Miskar W3 (uppermost Abiod and the base of the El Haria formations only) and Miskar W2, were analysed for carbon and oxygen stable isotopes. Sampling was undertaken following a nominal 1 m spacing interval in the cores. Narrower intervals were employed when significant lithological or sedimentological

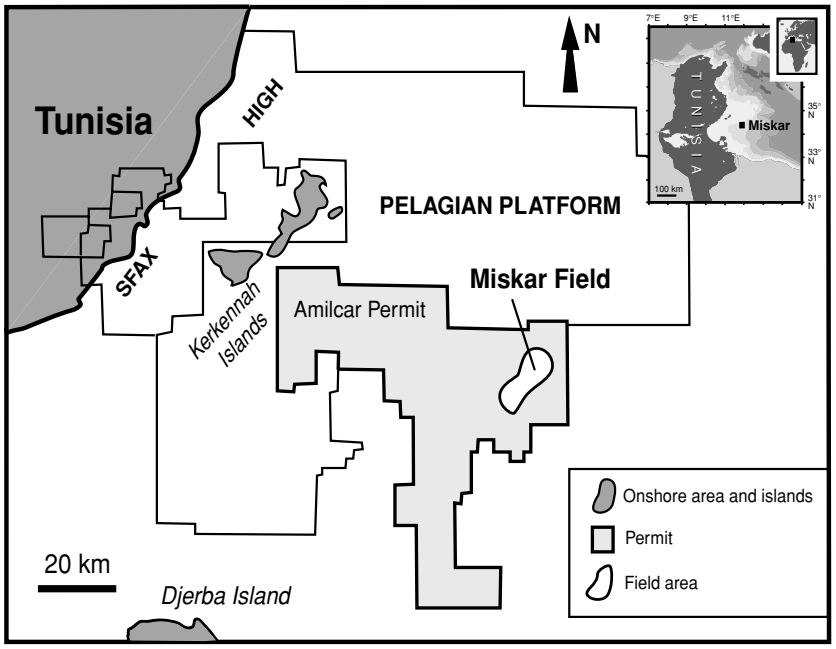

Fig. 2. Location map of the Miskar Field within the Amilcar permit and the Gulf of Gabes (modified from British Gas (1990)).

variation needed to be characterized. For example, in addition to the regular samples, all prominent marl seams were sampled.

LITHOSTRATIGRAPHY AND BIOSTRATIGRAPHY

The general Miskar Abiod facies is a wackestone to packstone rich in planktonic foraminifera, which constitute up to 35% of the rock. Benthic foraminifera are infrequent and rarely reach 5% of the rock. Other bioclastic debris includes echinoderm and bivalve debris, all floating in a very fine-grained micrite matrix. Similar facies characterize the formation onshore (Negra, 1994; Jarvis *et al*., 2002; Mabrouk, 2003; Mabrouk *et al*., 2005). Lithostratigraphic and sedimentological analysis of the uppermost part of the Aleg Formation and the Abiod Formation in the Miskar W1, W2 and W4 wells, and the uppermost part of the Abiod Formation and the base of the El Haria Formation in Miskar W3, has permitted the subdivision of the formation (Mabrouk, 2003) into two units in Miskar W3, into three units in Miskar W4, and into four units in the Miskar W1 and W2 wells (Fig. 4).

Biostratigraphic studies carried out by Moody *et al*. (1995) on Miskar W3, de Cabrera (in Mabrouk, 2003; Mabrouk *et al*., 2005) on Miskar W2, and Bailey *et al*. (2000a, b) on all four wells, have allowed the attribution of a probable Late Turonian-Coniacian age to the uppermost Aleg Formation, an Early Campanian-earliest Maastrichtian age to the Abiod Formation, and an Early Maastrichtian age to the base of the El Haria Formation

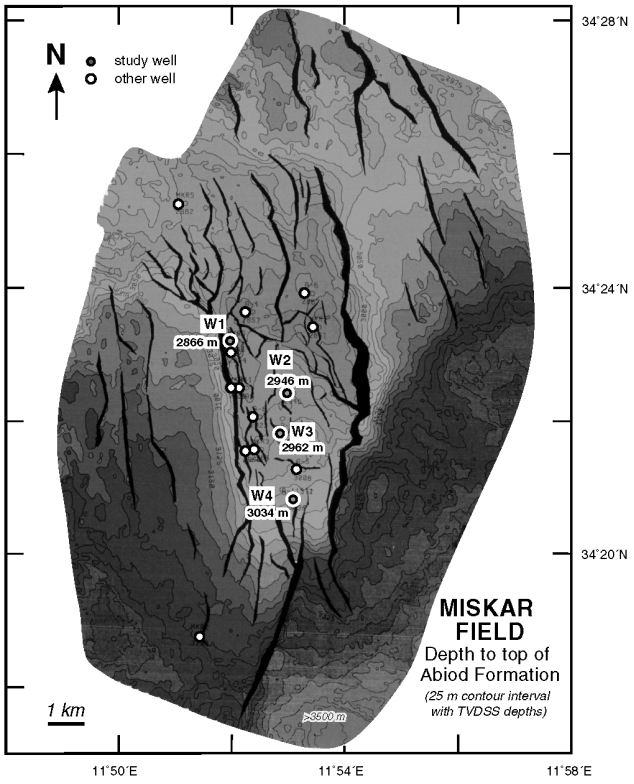

Fig. 3. Structural map showing the depth to the top of the Abiod Formation and major faults affecting the formation in the Miskar Field (British Gas, unpublished data).

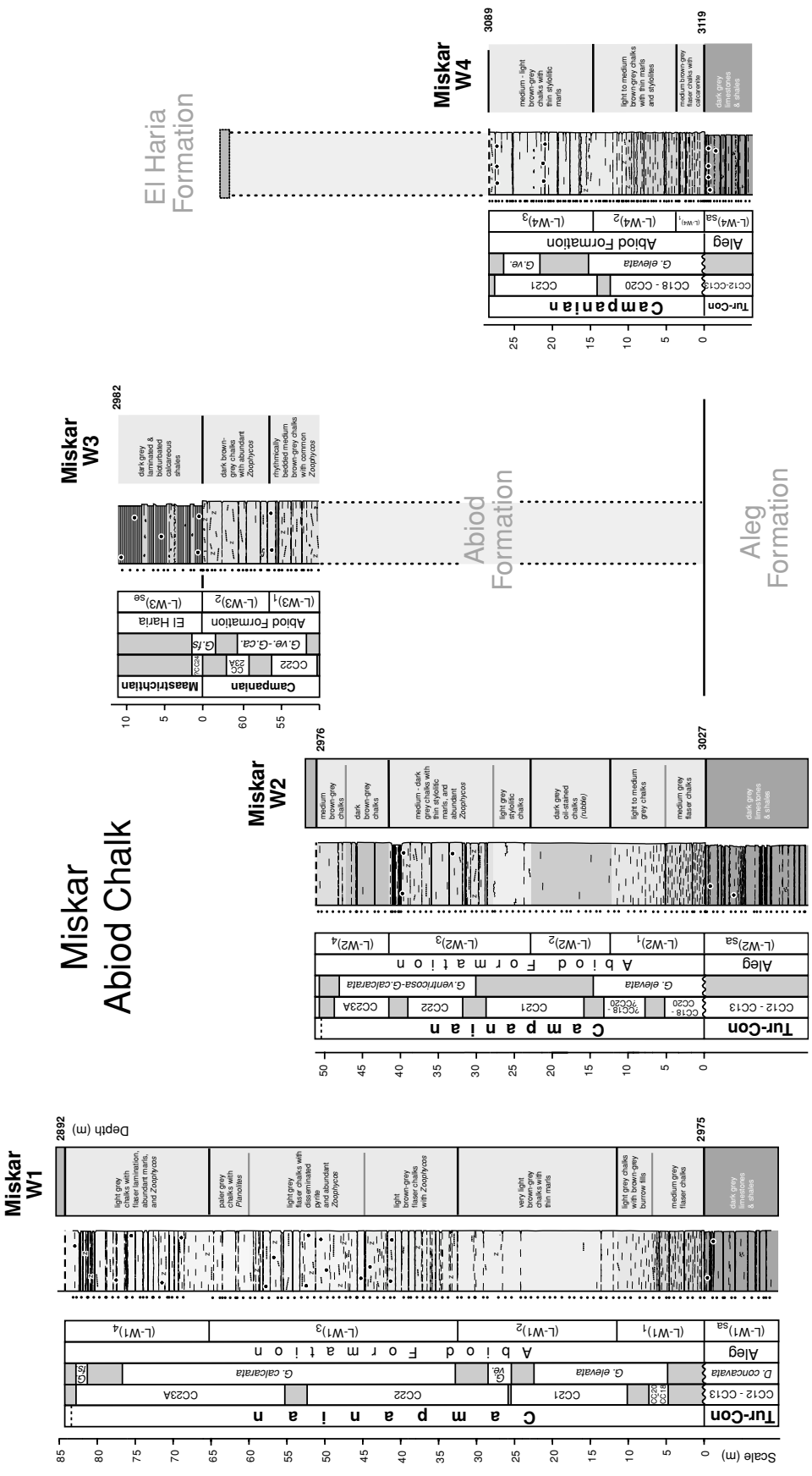

Fig. 4. Lithostratigraphic summary and biostratigraphic zonation of the Miskar W1, W2, W3 and W4 wells. Biostratigraphy after Bailey et al. (2000a).

Table 1. Major- and trace-element concentrations (μg/g) in five matrix-matched multi-element calibration solutions (AMI-1–5)

Element	Solution				
	AMI-1	AMI-2	AMI-3	AMI-4	AMI-5
Ti	2	5	20	100	180
Al	10	100	500	1000	1800
Fe	10	50	100	200	420
Mn	0.2	1	5	10	55
Mg	10	50	100	150	250
Ca	4000	3000	1000	500	35
Na	0.5	5	10	20	40
K	0.5	5	15	40	85
Ba	0.2	2	5	10	30
Cu	0.05	0.5	1	3	6
Li	0.05	0.2	0.5	1	2.5
Ni	0.05	0.5	1	2	5
Sr	4	10	30	60	110
Zn	0.1	1	10	25	50
V	0.2	0.4	1	2	4
Y	0.05	0.2	0.5	1	1.5

Whole-rock equivalent concentrations are found by multiplying the above values by 100, and in the case of the oxides, a further calculation based on the proportion of each element in its associated oxide.

(Fig. 4). Moreover, based on the palaeontological evidence, deposition occurred in a well-oxygenated outer-shelf to bathyal marine environment (Moody *et al*., 1995; de Cabrera in Mabrouk, 2003; Mabrouk *et al*., 2005; Bailey *et al*., 2000a, b).

METHODS

Strontium analysis

Analytical procedures followed Jarvis (1992), Jarvis and Jarvis (1992) and Totland *et al*. (1992). Oven-dried samples (0.5 g) were accurately weighed into 50 ml PTFE beakers and washed down into the base with a few ml deionised water. 10 ml AnaLaR 29 M HF and 4 ml AnaLaR 12 M $HClO_4$ were added, and the mixtures allowed to stand for at least 1 hour. Samples were heated on a hotplate at 200°C until near dryness was reached, i.e., a viscous paste could be seen in the beaker. The acid addition and evaporation stages were repeated twice more. At the end of the third evaporative stage, 4 ml $HClO_4$ were added and heated as before in order to drive off residual HF. Finally, 10 ml 5 M HNO_3 were added to the sample. This was warmed at 50–60°C until the paste dissolved. The solution was checked to make sure that all material had been digested, and then made up to volume in a 50 ml A-grade volumetric flask. In a few cases, a white precipitate formed on addition of the HNO_3. This necessitated adding 20–30 ml deionised water to the solution and warming until the precipitate dissolved. The final dilution factor was 1:100.

Table 2. Reproducibility and accuracy of strontium determinations: data for rock reference materials analysed with Miskar W1 samples

Reference material	Lithology	Strontium content (μg/g)		
		Mean	SD (σ_n)	Reference value
CCH-1	limestone	293	12	284
DWA-1	dolostone	36	1	49
JLs-1	limestone	287	4	296
KH-2	limestone	583	7	545
SCo-1	shale	181	2	174

Reference materials were prepared in the same way (Jarvis, 1992; Totland *et al*., 1992). Major elements excluding SiO_2, and a range of trace elements including Ba and Sr, were determined in the acid digests by inductive coupled plasma-atomic emission spectrometry (ICP-AES) for the four Miskar wells. Calibration was performed with matrix-matched multi-element standard solutions made from BDH single-element stock solutions (Table 1). One solution was used as an external drift monitor. Drift correction was performed using in-house software. Precision and accuracy were assessed by preparing and analysing a suite of sediment reference materials along with the samples. The reproducibility and accuracy of the strontium determinations was generally good (Table 2).

Carbon and oxygen stable-isotopes analyses

Samples were analysed in the stable isotope laboratory at Oxford University. The analytical procedure followed Jenkyns *et al*. (1994). Samples were cleaned using 10% H_2O_2 followed by acetone and then dried at 60°C. They were then reacted with purified orthophosphoric acid at 90°C and analyzed on-line using a VG Isocarb device and Prism mass spectrometer. Normal corrections were applied and the results are reported using the usual δ notation, in ‰ deviation from the VPDB (Vienna Pee Dee Belemnite) standard.

Strontium, $\delta^{13}C$ and $\delta^{18}O$ results are listed in Tables 3–9. Barium data are also reported (Tables 3–5) in order to identify samples that are potentially contaminated by drilling mud or contain diagenetic barite (see below). Data for other elements are presented in Mabrouk (2003).

RESULTS

Strontium results

The strontium contents for the Miskar W1 well correlate positively with carbonate (Table 3) with an average content around 1130 μg/g in the Abiod chalk samples and 918 μg/g in the Aleg limestone samples. This relationship is reversed when the few intercalating marl samples

Table 3. Carbonate and trace-element data for the Miskar W1 well

Depth (m)	Lithology	$CaCO_3$ (%)	Trace elements (μg/g)	
			Ba	Sr
2892.07	C	89.8	52	940
2892.52	C	90.1	50	1160
2893.17	C	88.9	41	1000
2893.95	C	92.6	43	989
2894.04	M	85.6	177	1727
2894.80	C	90.4	53	1090
2895.53	C	92.3	52	1070
2896.33	M	87.3	83	1320
2896.35	C	89.7	60	1210
2897.28	C	90.5	45	1010
2898.03	C	89.5	46	945
2899.02	M	89.9	57	1020
2899.08	C	92.8	41	924
2899.90	C	93.6	42	941
2900.90	C	93.2	49	1030
2901.30	M	90.6	68	1250
2901.78	C	93.6	47	960
2902.62	C	90.5	69	1220
2902.65	M	88.9	84	1340
2903.47	C	92.4	57	946
2904.50	C	88.0	58	1110
2904.70	M	86.1	75	1440
2905.12	C	88.5	88	1000
2905.80	C	90.6	48	977
2906.60	C	89.4	50	1100
2910.47	C	90.3	48	1060
2911.43	C	93.3	51	1030
2911.75	M	85.0	125	1720
2912.12	C	92.3	47	887
2912.78	C	93.9	50	959
2913.50	M	81.8	163	1880
2913.70	C	93.3	52	982
2914.50	C	93.1	51	930
2915.42	C	92.2	59	1090
2916.05	C	92.9	57	1100
2917.00	C	92.3	92	1120
2917.90	C	92.4	90	1080
2919.05	C	90.4	143	1220
2919.55	C	90.4	183	1280
2920.40	C	90.4	81	1290
2921.25	C	90.7	109	1090
2922.15	C	91.4	146	1140
2922.98	C	92.3	67	1177
2923.88	C	88.7	122	1230
2924.70	C	88.0	103	1550
2925.60	C	87.7	97	1400
2926.37	C	90.7	64	1350
2927.15	C	91.2	57	1310
2928.04	C	90.9	61	1370
2928.60	C	90.7	69	1450
2929.50	C	93.1	52	1260
2929.52	M	84.3	96	2040
2930.35	M	85.1	87	1760
2931.18	C	88.9	64	1450
2932.18	C	90.7	84	1560
2933.03	C	90.3	1370	1420
2933.88	C	87.5	1160	1590
2934.40	C	90.6	734	1280
2935.65	C	92.6	48	1130
2936.30	M	87.0	74	1380
2936.60	C	93.4	182	1110
2937.40	C	93.7	54	1200
2938.20	C	93.0	57	1130
2939.10	C	93.1	49	1030
2939.85	M	89.2	89	1420
2940.75	M	88.8	57	1430
2941.50	C	94.3	69	1110
2942.74	M	90.0	63	1280
2943.27	C	94.9	37	990
2944.25	C	96.7	89	875
2945.00	C	95.1	43	995
2945.03	M	86.5	82	1590
2946.16	C	93.9	51	1020
2946.68	M	89.6	72	1430
2948.14	C	96.3	78	833
2949.05	C	94.7	36	889
2949.87	C	96.2	61	1010
2951.08	M	85.5	523	1780
2951.63	C	95.4	164	1030
2952.43	C	92.7	415	966

Carbonate values calculated from Ca elemental determinations assuming that all Ca occurs in carbonate; C = chalk, M = marl.

are included, as anomalously high Sr contents occur (e.g., 4260 μg/g at the Abiod/Aleg boundary) within some marl seams (Table 3). This increase in Sr is not coincident with a similar increase in $CaCO_3$, overshadowing their positive relationship, and misleadingly suggests that Sr is lowest when Ca is highest. These samples are commonly marl samples that are also rich in barium, pointing to a geochemical association with barite. In fact, anomalously high concentrations of Ba were obtained in some Miskar W1 samples (up to 1930 μg/g at the Aleg/Abiod boundary); although the average is 297 μg/g in the Abiod samples and 227 μg/g in the Aleg samples (Table 3).

The Miskar W1 well was drilled employing a water-based fluid, but the use of a barite mud-weight means that there is a possibility of Ba-contamination, particularly within the uppermost 25 m of the Abiod Formation which is characterised by high porosities and where infiltration by the drilling fluid is more likely. However, great care was taken to avoid the outer parts of the core which might be contaminated by the drilling fluid, and Ba generally displays a low average concentration of 60 μg/g in the upper beds. Nonetheless, the presence of barite remains the most likely explanation for the anomalous high values obtained for some samples, especially with

Table 3. (continued)

Depth (m)	Lithology	$CaCO_3$ (%)	Trace elements (μg/g)	
			Ba	Sr
2953.33	C	95.4	324	904
2954.17	C	95.9	1420	918
2954.92	C	96.7	1310	952
2955.63	C	94.7	1280	1120
2956.50	C	94.7	582	1070
2957.50	C	96.3	526	1050
2958.14	C	97.6	601	968
2959.05	C	95.5	697	982
2959.87	C	95.7	884	1040
2960.68	C	95.9	552	989
2961.65	C	95.2	324	985
2961.68	M	68.7	336	1597
2962.38	C	96.6	513	927
2963.30	M	81.4	409	1470
2964.05	C	95.4	691	1060
2964.83	C	97.0	392	1020
2965.60	C	96.1	1270	996
2966.77	C	95.3	835	1080
2967.55	C	93.6	550	1210
2968.55	C	91.9	153	1410
2969.35	C	90.6	269	1410
2970.28	C	92.5	291	1210
2970.65	M	85.5	290	1860
2971.28	C	92.3	1070	1290
2973.10	C	88.7	551	1460
2973.75	C	87.3	671	1660
2974.78	C	85.9	710	1350
2975.28	M Aleg/Abiod	0.6	192	4260
2976.38	C	90.1	1930	1090
2976.92	C	91.8	40	904
2977.75	M	30.0	131	1810
2977.95	C	93.7	31	891
2978.88	C	91.1	59	842
2979.35	M	33.8	101	2700
2980.58	C	94.6	30	854
2981.55	C	94.8	63	858
2982.45	C	91.1	72	851
2983.11	C	87.7	61	1030
2983.42	M	25.8	102	1650
2983.90	C	89.3	139	945

the increase of Sr in samples where Ba is high, as barite typically contains high Sr. The occurrence of diagenetic barite offers an alternative explanation to contamination for these anomalously high values. Excluding these anomalous high concentrations, the Ba/Al profile shows more systematic variation that is independent of lithology (Fig. 5).

Strontium contents of the Miskar W2 average around 1300 μg/g in the Abiod chalk samples and 984 μg/g in the Aleg chalk samples but show a considerable increase in the Abiod marls (Table 4, Fig. 5). At these levels Sr sometimes reaches 0.9%. The Sr/Al profile is similar in shape to that of Mg/Al (Mabrouk, 2003) and broadly follows $CaCO_3$, which suggests a close relationship between Sr and Mg and their incorporation predominantly in calcite. The average barium content in the Miskar W3 Abiod samples is 682 μg/g with some abnormal concentrations of about 1.2%. In this case, contamination of samples by drilling mud or the presence of diagenetic barite are necessary to reach such high concentrations, especially as excursions on the Ba/Al profile correlate with those in Sr/Al (Mabrouk, 2003).

The strontium contents of the Miskar W3 samples average 1790 μg/g in all Abiod samples and 1710 μg/g in the overlying El Haria Formation samples. Some anomalously high values are encountered in both formations in both chalk and marl samples (up to 3230 μg/g in the El Haria and 7540 μg/g in the Abiod). The Sr/Al geochemical trend is similar to those of $CaCO_3$ and Mg/Al, with the exception of some spikes where strontium concentrations are unusually high (Mabrouk, 2003), and which coincide with high barium values (Table 5).

The average Sr contents in the Miskar W4 well are around 970 μg/g in the Abiod Formation chalk samples and around 780 μg/g in the Aleg limestone samples. Marl samples exhibit contents that are usually higher (Table 6). On the other hand, one or two chalk samples contain more than 0.2% of Sr; these correlate with abnormally high barium values (above 1%).

$\delta^{13}C$ and $\delta^{18}O$ results

In the Miskar W1 well, the uppermost part of the Aleg Formation (2983.90–2975.28 m depth) shows an average of 1.96‰ $\delta^{13}C$ and –4.96‰ $\delta^{18}O$ (Table 7). Carbon isotopes in the formation range from 2.11–1.75‰ (Fig. 5). The isotopic signatures of the contact between the Aleg and the Abiod Formations (2975.28 m) are 2.06‰ and –4.50‰ for $\delta^{13}C$ and $\delta^{18}O$, respectively. The Abiod Formation, above, has an average of 2.13‰ $\delta^{13}C$ and –4.33‰ $\delta^{18}O$. The carbon isotope signal varies between 2.38–1.85‰, whereas oxygen isotopes range from –3.62‰ and –4.98‰ (Table 7, Fig. 5).

Within the Miskar W4 well, the average isotopic content of the Aleg Formation (4906.32–4896.91 m depth) is 2.07‰ for carbon and –5.44‰ for oxygen. Carbon isotopes range from 2.21–1.94‰ (Table 8, Fig. 5), whereas oxygen isotopes display values of –4.97‰ to –5.92‰. At the contact between the Aleg and the Abiod formations, values are 2.09‰ $\delta^{13}C$ and –5.43‰ $\delta^{18}O$ (Table 8). Above this, the Abiod Formation displays a slightly different range of isotopic values with an average of 2.13‰ $\delta^{13}C$ and an average of –5.13‰ $\delta^{18}O$. In this well, the formation contains carbon and oxygen isotope maxima of 2.38‰ and –4.25‰ respectively, and carbon and oxygen isotope minima of 1.86‰ and –5.76‰.

Only a few selected samples from the Miskar W2 and W3 wells were analyzed for carbon and oxygen isotopes.

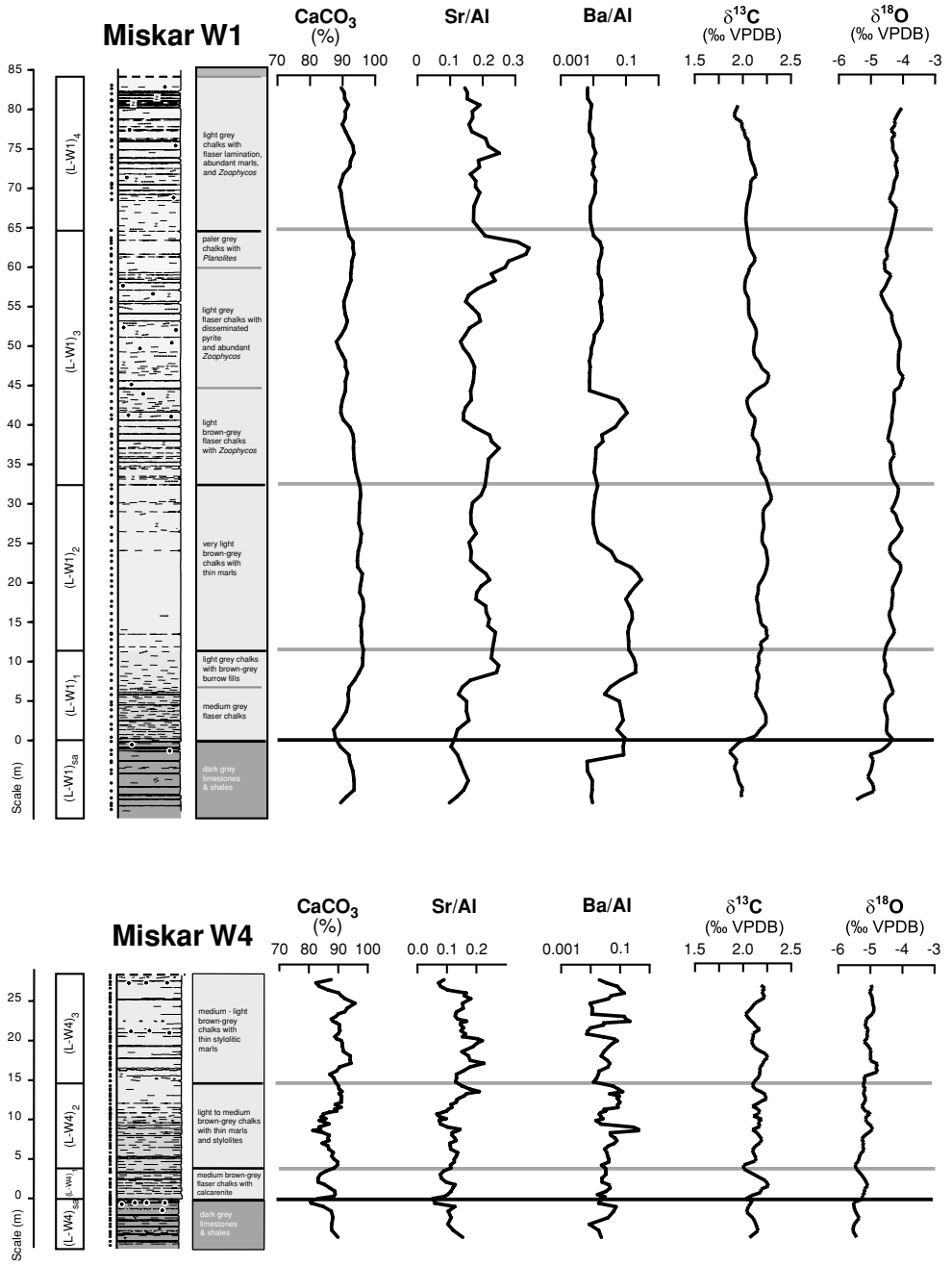

Fig. 5. Stratigraphic variation in $CaCO_3$, Sr/Al, Ba/Al, $\delta^{13}C$, and $\delta^{18}O$ through the Miskar W1 and W4 wells. Strontium and Ba are normalised to aluminium. Plots are three-point-moving-averages of chalk sample data only. Long horizontal black line is the geochemical boundary between the Aleg and Abiod formations, grey lines are boundaries between Abiod lithological units (Mabrouk, 2003; Mabrouk et al., 2005), shown to the left of the lithology column.

Results are shown in Table 9. The Miskar W2 samples average 2.12‰ $\delta^{13}C$ and –5.05‰ $\delta^{18}O$. The Miskar W3 samples have lighter average carbon (1.62‰), but heavier average oxygen (–4.66‰) values. Two of the Miskar W2 Aleg samples again have lighter $\delta^{18}O$ values than those from the Abiod together with lower strontium contents (Table 4). One of the Miskar W2 Abiod samples has the highest carbon isotope value (2.52‰) recorded in the four wells, but the significance of this is uncertain due to a lack of other data from the well. One analyzed Miskar W3 Abiod sample shows similar $\delta^{18}O$, $\delta^{13}C$, and Sr contents to those of the Miskar W1 and W4 wells (Tables 3,

Table 4. Carbonate and trace-element data for the Miskar W2 well

Depth (m)	Lithology	$CaCO_3$ (%)	Trace elements (μg/g)	
			Ba	Sr
2975.02	C	88.6	22	899
2975.43	C	90.1	33	925
2976.18	C	89.4	33	882
2976.94	C	92.5	28	907
2977.76	C	89.1	36	1330
2978.39	C	88.9	34	1070
2979.25	C	89.8	36	1210
2980.03	M	47.6	128	7380
2980.14	M	33.5	420	8830
2980.72	C	92.3	37	1140
2981.50	C	91.8	27	905
2982.50	M	72.5	24	902
2982.98	C	92.9	34	942
2983.84	C	93.1	172	934
2984.64	C	88.4	330	1360
2984.83	M	48.2	402	6190
2985.18	M	49.6	486	5410
2985.60	C	88.1	291	1210
2985.74	C	46.5	311	5340
2985.96	C	33.8	245	6400
2986.91	C	89.0	262	1220
2987.70	C	88.8	460	1580
2988.54	C	87.3	494	1400
2989.25	C	88.9	596	1390
2989.93	M	55.6	401	1680
2990.98	C	89.0	579	1350
2991.59	C	91.0	3070	1440
2992.34	M	79.1	384	2150
2993.16	C	89.8	459	984
2993.82	C	90.0	474	945
2994.42	M	38.7	415	8890
2995.33	C	90.7	318	1150
2995.91	C	91.4	252	1120
2996.65	C	92.0	248	3360
2997.36	C	91.9	178	1190
2998.05	C	95.0	516	889
2998.35	C	96.3	35	858
2999.12	C	94.5	458	909
2999.93	C	92.1	83	812
3000.71	C	94.0	169	1010
3001.48	C	95.0	288	998
3002.19	C	92.9	339	1020
3002.98	C	94.0	126	928
3003.81	C	95.0	1040	895
3004.65	C	94.8	838	895
3005.42	C	94.4	168	814
3006.20	C	94.0	1390	877
3007.17	C	90.8	498	839
3007.83	C	94.0	479	941
3008.35	C	94.7	593	770
3009.39	C	90.9	686	838
3010.41	C	93.0	325	857
3010.95	C	89.7	7590	1180
3011.76	C	94.1	510	928
3012.26	C	84.4	12700	1360
3013.33	M	81.0	9970	1760
3014.15	C	89.0	532	1090
3014.71	C	90.8	573	1050
3015.97	C	90.7	806	983
3016.76	C	90.0	245	989
3017.60	C	91.4	272	893
3018.24	M	76.8	822	4010
3019.28	C	88.1	301	1230
3019.90	C	89.2	308	1130
3020.86	M	48.0	1300	2410
3021.68	C	87.9	187	1040
3022.38	C	87.7	241	1110
3023.20	C	79.0	720	4500
3023.72	C	89.4	299	884
3024.43	M	69.5	271	7540
3024.67	C	88.5	231	941
3025.53	C	80.8	301	862
3026.12	C	84.8	335	935
3026.14	M Aleg/Abiod	2.1	139	766
3026.34	C	75.1	212	3100
3027.19	M	63.9	100	1100
3027.73	M	47.8	160	1020
3028.51	M	30.5	82	1850
3029.53	C	85.8	31	786
3030.13	M	50.5	220	1020
3030.92	M	44.2	64	944
3031.48	M	43.8	138	999
3032.59	C	79.5	59	926
3032.94	C	88.5	35	795
3033.43	M	43.9	319	1340
3034.26	M	20.1	106	1810
3034.84	M	60.8	117	1380
3035.59	C	90.5	152	655
3036.34	M	26.5	260	2250
3036.95	C	88.7	118	632
3037.92	M	16.0	584	4180
3038.63	M	47.9	2310	2430
3039.19	C	86.6	92	608
3039.33	M	31.5	584	6580

Carbonate values calculated from Ca elemental determinations assuming that all Ca occurs in carbonate; C = chalk, M = marl.

4, 9). One of the El Haria samples of Miskar W3 has carbon and oxygen isotope values comparable to those of the Abiod, whereas the other shows the lightest carbon isotope value (1.21‰) registered in all wells; this might be attributed to contamination with oil.

DISCUSSION

The stable-isotope crossplots for the Miskar wells (Figs. 6 and 7) show a clear separation between the Abiod and the Aleg samples manifested particularly in their oxy-

Table 5. Carbonate and trace-element data for the Miskar W3 well

Depth (m)	Lithology	$CaCO_3$ (%)	Trace elements (μg/g)	
			Ba	Sr
2981.76	M	31.5	137	1330
2982.83	M	34.8	115	1690
2983.74	M	35.9	110	1600
2984.54	M	64.9	141	1430
2985.75	M	40.9	145	1510
2986.35	M	20.0	123	1860
2987.10	M	31.5	125	1440
2987.60	M	31.1	201	1580
2988.45	M	48.4	95	1490
2989.53	M	35.4	106	1690
2990.51	M	36.0	98	1340
2990.93	M	28.8	117	2150
2991.82	M	10.1	140	3050
2992.01	M Abiod/El Haria	26.1	188	3230
2992.05	M	42.8	69	1030
2992.11	M	65.8	117	1150
2992.65	M	46.9	84	1440
2992.70	C	79.1	94	1210
2993.30	C	82.7	46	1240
2993.70	C	92.4	112	1270
2994.47	C	76.2	246	1440
2995.04	C	79.3	7230	1770
2996.04	C	82.8	501	1510
2996.87	M	71.8	310	2740
2996.94	C	83.0	330	1400
2997.48	C	87.2	1030	1330
2997.95	M	79.2	142	2820
2998.01	C	83.8	51	1400
2998.57	C	90.2	210	1220
2999.07	C	88.6	128	1320
2999.83	M	57.0	1040	7540
2999.92	C	84.5	806	1390
3000.79	M	80.6	83	1400
3001.00	M	80.8	83	1000
3001.74	C	79.7	75	1520
3002.33	M	78.8	62	1540
3002.36	C	81.4	48	1970
3002.81	C	77.7	750	1420
3003.52	C	78.3	7330	2200
3004.00	M	68.7	369	2730
3004.64	M	79.9	353	1700
3004.71	C	86.6	363	1470
3005.46	M	78.7	535	2450
3005.69	C	85.7	504	1490
3006.30	C	85.5	1050	1410
3006.73	C	87.8	493	1400
3007.26	C	84.4	2150	1600
3007.68	C	84.5	299	1290

Carbonate values calculated from Ca elemental determinations assuming that all Ca occurs in carbonate; C = chalk, M = marl.

gen isotope compositions. The Aleg samples are lighter in $\delta^{18}O$ which would indicate *a priori*, a greater burial diagenetic effect for the Formation. Depletion in $\delta^{18}O$ through burial diagenesis has been demonstrated by numerous previous studies (e.g., Scholle, 1974, 1977; Mimran, 1978; Jørgensen, 1986, 1987) as being a consequence of re-equilibration of the carbonate phase with the interstitial water and the imposed geothermal gradient. Jørgensen (1987) pointed out that lower $\delta^{18}O$ values, generated by the temperature-induced isotopic re-equilibration of chalk with increasing depth, are highly influenced by deep-burial derived chemical processes (pressure-dissolution, precipitation of calcite cement, recrystallisation and ion-exchange).

However, both $\delta^{13}C$ and $\delta^{18}O$ isotopes values recorded in our samples display a significant negative shift at the Aleg-Abiod boundary, which cannot be interpreted as being solely a consequence of burial diagenetic effects. Mabrouk (2003) assumed that the two formations were subject to "homogenous burial". In this case, the oxygen isotope contents of the two formations should fall within the same values range. However, both the carbon and oxygen isotopes signatures for the Aleg Formation are found to be significantly shifted towards lighter values compared to the Abiod samples.

Average Sr contents in the Abiod formation of around 1000–1200 μg/g are typical of unaltered chalks. However, strontium-$\delta^{18}O$ crossplots for the Miskar wells (Figs. 6 and 7) show that the Aleg samples can again be differentiated from the Abiod samples, with lower strontium contents and lower $\delta^{18}O$ values. This is most clearly expressed on Fig. 6 for the W1 Miskar well, which shows the Aleg samples to be entirely separated from the Abiod samples. This separation is not seen in data from the W2–W4 wells (Fig. 7), although once again Sr tends to be lower in the Aleg samples.

Depletion in strontium has been documented elsewhere as being a consequence of burial diagenesis (Renard, 1972, 1986; Jørgensen; 1981; Malone *et al.*, 1990; Morse and McKenzie, 1990; Apitz, 1991; McCorkle *et al.*, 1995), which induces a short-term Sr loss leading to the chemical stabilization of the original carbonates. Nevertheless, if it is assumed that only burial diagenesis has caused lighter oxygen isotope values, two geochemical results should accompany this: (1) a similar range of oxygen isotope values for both formations, as their lithostatic load is very similar (the Abiod Formation is only around 85 m thick); (2) similarly low Sr contents in both formations.

Accordingly, the shift to lower Sr values, coupled to depletion in $\delta^{13}C$ and $\delta^{18}O$ in the Aleg sediments, is probably due to another geological factor that has affected the Aleg formation prior to the deposition of the Abiod sediments. Similar geochemical signatures have been documented by Land (1979, 1986) in his work on Jamaican Miocene chalks and on Shatsky Rise limestones (DSDP), and these were interpreted as being a result of

Table 6. Carbonate and trace-element data for the Miskar W4 well

Depth (m)	Lithology	$CaCO_3$ (%)	Trace elements (μg/g)	
			Ba	Sr
3089.52	C	92.7	92	796
3089.88	C	90.4	101	827
3090.31	M	79.3	98	1360
3090.35	C	79.6	330	777
3090.72	C	77.2	694	661
3091.16	C	93.7	1300	784
3091.76	C	88.9	247	771
3091.82	C	87.9	422	796
3092.16	C	96.1	89	851
3092.40	M	89.9	57	813
3092.58	M	88.3	90	1000
3092.92	C	92.8	26	786
3093.45	M	87.9	49	932
3093.54	C	98.2	45	930
3094.09	C	87.9	122	853
3094.17	C	90.6	74	1050
3094.40	C	91.4	47	946
3094.95	C	85.9	2840	749
3095.18	C	85.6	71	878
3095.21	C	92.9	378	945
3095.60	C	89.6	45	822
3095.95	C	88.7	57	814
3096.23	M	89.4	119	1210
3096.31	C	92.6	55	841
3096.73	C	90.4	43	1210
3097.12	C	86.9	33	845
3097.18	M	92.2	108	1060
3097.35	C	89.2	437	924
3097.51	C	92.1	336	856
3097.82	C	91.9	182	854
3098.33	M	89.4	257	1080
3098.37	C	90.1	190	900
3098.42	M	84.5	1540	1010
3098.72	C	92.3	187	820
3099.10	M	85.6	135	781
3099.36	M	93.0	119	960
3099.77	C	74.1	810	2320
3099.92	M	87.1	269	971
3099.97	C	96.9	42	861
3100.38	C	92.2	393	843
3100.67	M	91.0	43	852
3100.89	C	93.9	70	859
3101.31	M	85.0	191	1340
3101.33	C	85.6	82	820
3101.89	C	88.9	198	1110
3102.16	C	86.9	94	777
3102.71	M	87.7	312	1340
3102.75	C	89.7	69	1110
3103.32	C	90.4	110	927
3103.70	C	90.1	917	846
3103.89	C	90.2	277	905
3104.28	C	93.5	359	915
3104.50	C	87.1	190	1330
3104.73	C	92.8	1410	1020
3105.13	C	93.6	173	867
3105.15	C	86.3	298	909
3105.59	C	93.5	1630	1050
3106.04	C	87.1	203	987
3106.22	C	92.3	407	1070
3106.27	M	84.7	340	1140
3106.30	C	86.8	194	888
3106.70	C	89.4	418	1180
3106.73	C	84.3	196	1010
3106.84	M	88.1	217	1150
3106.91	C	81.0	324	970
3107.24	C	89.0	431	1140
3107.27	C	82.6	127	879
3107.55	C	85.6	287	1110
3107.93	C	82.4	208	1040
3108.63	C	92.5	438	1060
3108.70	C	75.5	10700	1950
3108.76	C	84.1	243	944
3109.12	C	84.5	678	955
3109.49	C	85.7	178	914
3109.55	M	78.8	446	951
3109.74	C	90.6	338	1030
3110.09	C	83.3	1030	991
3110.51	C	86.5	426	1020
3110.79	C	83.9	263	1000
3111.10	C	89.3	377	1030
3111.65	C	87.1	147	922
3112.14	C	88.6	256	1030
3112.47	C	87.7	461	1060
3112.78	C	89.5	349	1070
3113.14	C	92.1	44	488
3113.67	C	87.6	96	788
3113.95	C	85.9	494	974
3114.09	M	68.1	523	1940
3114.14	C	84.6	447	1090
3114.94	M	32.2	255	6800
3114.97	C	81.2	347	991
3115.38	C	83.5	102	942
3115.62	C	84.7	332	1120
3115.97	C	87.9	570	1030
3116.58	C	88.6	326	1060
3116.91	C	90.1	69	1220
3117.18	C	88.1	101	689
3117.32	C	86.9	704	764
3117.48	M Aleg/Abiod	47.0	526	894
3117.70	C	74.8	92	751
3117.90	M	24.7	122	1220
3118.08	C	80.1	42	698
3118.16	C	87.5	560	737
3118.64	M	38.4	293	1020
3119.00	C	87.2	653	754
3119.39	M	45.5	137	1240
3119.82	C	88.1	78	747
3120.12	M	39.6	1020	1300
3120.56	C	89.3	36	760
3120.90	M	42.6	81	996
3121.47	C	85.8	84	763
3121.79	M	54.0	155	1050
3122.12	C	88.1	269	1010
3122.72	M	46.3	150	1330
3123.22	C	95.8	44	887

Carbonate values calculated from Ca elemental determination assuming that all Ca occurs in carbonate; C = chalk, M = marl.

Table 7. Carbon and oxygen stable-isotope data for the Miskar W1 well

Depth (m)	Lithology	Isotope (‰VPDB)		Depth (m)	Lithology	Isotope (‰VPDB)		Depth (m)	Lithology	Isotope (‰VPDB)	
		$\delta^{13}C$	$\delta^{18}O$			$\delta^{13}C$	$\delta^{18}O$			$\delta^{13}C$	$\delta^{18}O$
2892.07	C	1.91	–4.01	2921.25	C	2.14	–4.36	2953.33	C	2.25	–4.07
2892.52	C	1.99	–4.00	2922.15	C	2.15	–4.16	2954.17	C	2.24	–4.07
2893.17	C	1.96	–4.12	2922.98	C	2.13	–4.14	2954.92	C	2.21	–4.35
2893.95	C	1.85	–4.31	2923.88	C	2.14	–4.05	2955.63	C	2.16	–4.29
2894.04	M	1.93	–4.17	2924.70	C	2.10	–4.05	2956.50	C	2.10	–4.37
2894.80	C	1.99	–4.34	2925.60	C	2.10	–4.34	2957.50	C	2.21	–4.26
2895.53	C	2.04	–4.22	2926.37	C	2.16	–4.04	2958.14	C	2.12	–4.41
2896.33	M	1.96	–4.59	2927.15	C	2.23	–4.06	2959.05	C	2.17	–4.39
2896.35	C	2.05	–3.90	2928.04	C	2.21	–4.30	2959.87	C	2.20	–4.51
2897.28	C	2.05	–4.59	2928.60	C	2.37	–3.62	2960.68	C	2.18	–4.30
2898.03	C	2.08	–4.47	2929.50	C	2.20	–4.29	2961.65	C	2.20	–4.16
2899.02	M	2.05	–3.90	2929.52	M	2.16	–4.35	2961.68	M	2.38	–4.33
2899.08	C	2.08	–4.31	2930.35	M	2.13	–4.21	2962.38	C	2.14	–4.46
2899.90	C	2.11	–4.31	2931.18	C	2.01	–4.29	2963.30	M	2.26	–4.46
2900.90	C	2.07	–4.14	2932.18	C	1.99	–4.31	2964.05	C	2.14	–4.65
2901.30	M	2.18	–4.17	2933.03	C	2.14	–4.35	2964.83	C	2.20	–4.56
2901.78	C	2.13	–4.21	2933.88	C	2.10	–4.40	2965.60	C	2.13	–4.61
2902.62	C	2.10	–4.30	2934.40	C	2.15	–4.28	2966.77	C	2.19	–4.47
2902.65	M	2.03	–4.33	2935.65	C	2.09	–4.52	2967.55	C	2.12	–4.65
2903.47	C	2.11	–4.23	2936.30	M	2.06	–4.52	2968.55	C	2.21	–4.20
2904.50	C	2.09	–4.41	2936.60	C	2.15	–4.39	2969.35	C	2.11	–4.28
2904.70	M	2.01	–4.57	2937.40	C	2.21	–4.07	2970.28	C	2.14	–4.40
2905.12	C	2.09	–4.28	2938.20	C	2.13	–4.50	2970.65	M	2.15	–4.77
2905.80	C	2.06	–4.10	2939.10	C	2.18	–4.23	2971.28	C	2.19	–4.51
2906.60	C	1.97	–4.22	2939.85	M	2.14	–4.47	2973.10	C	2.25	–4.45
2910.47	C	2.07	–4.54	2940.75	M	2.23	–4.48	2973.75	C	2.28	–4.52
2911.43	C	2.10	–4.42	2941.50	C	2.22	–4.12	2974.78	C	2.21	–4.56
2911.75	M	2.04	–4.62	2942.74	M	2.26	–4.25	2975.28	M Aleg/Abiod	2.06	–4.50
2912.12	C	2.13	–4.46	2943.27	C	2.31	–4.05	2976.38	C	2.11	–3.92
2912.78	C	2.17	–4.35	2944.25	C	2.27	–4.18	2976.92	C	1.75	–4.91
2913.50	M	2.09	–4.98	2945.00	C	2.32	–4.42	2977.75	M	1.83	–5.19
2913.70	C	2.06	–4.35	2945.03	M	2.25	–4.24	2977.95	C	2.01	–5.03
2914.50	C	2.05	–4.41	2946.16	C	2.13	–4.45	2978.88	C	1.89	–4.58
2915.42	C	2.05	–4.36	2946.68	M	2.25	–4.00	2979.35	M	1.94	–5.24
2916.05	C	1.99	–4.64	2948.14	C	2.25	–4.02	2980.58	C	1.91	–5.18
2917.00	C	2.04	–4.67	2949.05	C	2.15	–4.03	2981.55	C	1.96	–4.90
2917.90	C	2.05	–4.79	2949.87	C	2.21	–4.45	2982.45	C	2.02	–4.71
2919.05	C	2.11	–4.34	2951.08	M	2.24	–4.72	2983.11	C	2.02	–5.13
2919.55	C	2.01	–4.35	2951.63	C	2.27	–4.09	2983.42	M	1.90	–5.92
2920.40	C	2.05	–4.36	2952.43	C	2.26	–4.09	2983.90	C	2.07	–5.33

C = chalk, M = marl.

alteration in a vadose meteoric environment, due to the fact that meteoric waters are generally impoverished in strontium, $\delta^{13}C$ and $\delta^{18}O$ (e.g., Faure, 1986; Renard, 1986; Morse and Mackenzie, 1990). By analogy, it can be argued that the uppermost Aleg Formation has been subject to surface diagenetic alteration as a result of a subaerial exposure prior to the deposition of the Abiod chalk. This argument is consistent with the biostratigraphic study of Bailey *et al*. (2000a, b) who proposed that an unconformity exists between the top Aleg (Turonian-Coniacian age) and the basal Abiod (Campanian age) formations in the Miskar Field.

Assuming that the oxygen isotope values have been shifted from their primary palaeo-oceanic signature through burial diagenesis in the Abiod formation, and through both burial and meteoric diagenesis in the Aleg formation, then their use as marine palaeotemperature indicators should be considered as unreliable. Such a conclusion is clearly supported by our attempt to use the oxygen isotopes to determine the palaeotemperatures of the water column during the Late Cretaceous, using the temperature equation (Epstein *et al*., 1953; Craig, 1965; Anderson and Arthur, 1983):

Table 8. Carbon and oxygen stable-isotope data for the Miskar W4 well

Depth (m)	Lithology	Isotope (‰VPDB)		Depth (m)	Lithology	Isotope (‰VPDB)	
		$\delta^{13}C$	$\delta^{18}O$			$\delta^{13}C$	$\delta^{18}O$
3089.52	C	2.07	–4.90	3106.22	C	2.21	–5.10
3089.88	C	2.25	–4.85	3106.27	M	2.24	–4.97
3090.35	C	2.17	–5.22	3106.30	C	1.99	–5.03
3090.72	C	2.21	–4.78	3106.84	M	2.18	–5.07
3091.16	C	2.15	–5.13	3106.91	C	2.10	–5.29
3092.58	M	2.26	–4.95	3107.55	C	2.25	–5.13
3092.92	C	1.92	–4.74	3107.93	C	2.07	–4.97
3093.54	C	2.00	–4.99	3108.63	C	2.16	–4.82
3094.40	C	2.10	–5.08	3108.76	C	2.00	–5.07
3094.95	C	2.04	–5.34	3109.12	C	2.24	–5.28
3095.18	C	2.16	–5.03	3109.74	C	2.22	–5.22
3095.60	C	2.16	–5.18	3110.09	C	2.09	–5.34
3095.95	C	2.17	–5.01	3110.51	C	2.17	–5.08
3096.73	C	1.96	–5.18	3111.10	C	2.08	–5.31
3097.35	C	2.16	–5.12	3111.65	C	1.99	–5.23
3097.51	C	2.09	–5.32	3112.14	C	2.24	–5.44
3097.82	C	2.02	–4.88	3112.47	C	2.14	–5.42
3098.33	M	2.18	–4.95	3112.78	C	1.97	–5.29
3098.72	C	2.25	–5.13	3113.67	C	1.86	–5.76
3099.10	M	2.25	–4.95	3113.95	C	2.13	–5.29
3099.77	C	2.22	–4.93	3115.38	C	2.38	–4.76
3099.97	C	2.14	–5.15	3115.62	C	2.16	–5.43
3100.38	C	2.22	–4.25	3115.97	C	2.21	–5.07
3100.89	C	2.11	–5.12	3116.58	C	2.14	–5.10
3101.89	C	2.15	–5.01	3116.91	C	2.16	–5.38
3102.16	C	2.17	–5.50	3117.18	C	1.91	–5.30
3102.75	C	1.97	–5.02	3117.32	C	2.04	–5.08
3103.32	C	2.10	–5.23	3117.48	M Aleg/Abiod	2.09	–5.43
3103.70	C	2.26	–5.23	3117.70	C	2.11	–5.50
3103.89	C	2.17	–5.23	3118.16	C	2.01	–5.65
3104.28	C	2.24	–5.18	3119.00	C	1.99	–5.44
3104.50	C	2.21	–5.15	3119.39	M	2.06	–5.31
3104.73	C	2.25	–5.12	3120.56	C	2.21	–5.33
3105.13	C	2.04	–5.27	3121.47	C	2.08	–5.92
3105.15	C	2.17	–5.20	3122.12	C	2.13	–5.43
3106.04	C	2.04	–5.36	3123.22	C	1.94	–4.97

C = chalk, M = marl.

$$t°C = 16.0 - 4.14(\delta_c - \delta_w) + 0.13(\delta_c - \delta_w)^2$$

where δ_c is the corrected $\delta^{18}O$ VPDB of CO_2 obtained from the carbonate by reaction with phosphoric acid at 25°C (the isotope composition of oxygen in carbonates samples is determined from CO_2 gas obtained by reacting samples with 100% phosphoric acid normally at 25°C), and δ_w is the corrected $\delta^{18}O$ VSMOW of CO_2 equilibrated isotopically at 25°C with the water from which the carbonate was precipitated.

Assumptions must be made regarding the isotopic composition of seawater (δ_w) because of the variation of $\delta^{18}O$ of seawater with time caused by continental glaciations and also by variations in salinity. Accordingly, if we take a $\delta^{18}O$ value of –1.0‰ VSMOW for non-glacial Late Cretaceous sea-water (δ_w), as assumed by

Table 9. Carbon and oxygen stable-isotope data for the Miskar W2 and W3 wells (selected samples only)

Well	Fmn	Depth (m)	Lithology	Isotope (‰VPDB)	
				$\delta^{13}C$	$\delta^{18}O$
W2	Ab	2982.98	C	2.51	–4.81
W2	Ab	3015.97	C	2.17	–5.09
W2	Al	3029.53	C	1.49	–3.91
W2	Al	3035.59	C	2.24	–5.68
W2	Al	3039.19	C	2.21	–5.77
W3	EH	2984.54	M	1.19	–4.48
W3	EH	2984.54	M	1.23	–4.43
W3	EH	2985.75	M	1.84	–4.88
W3	Ab	3004.64	M	2.20	–4.85

Fmn = Formation; Al = Aleg; Ab = Abiod; EH = El Haria; C = chalk; M = marl.

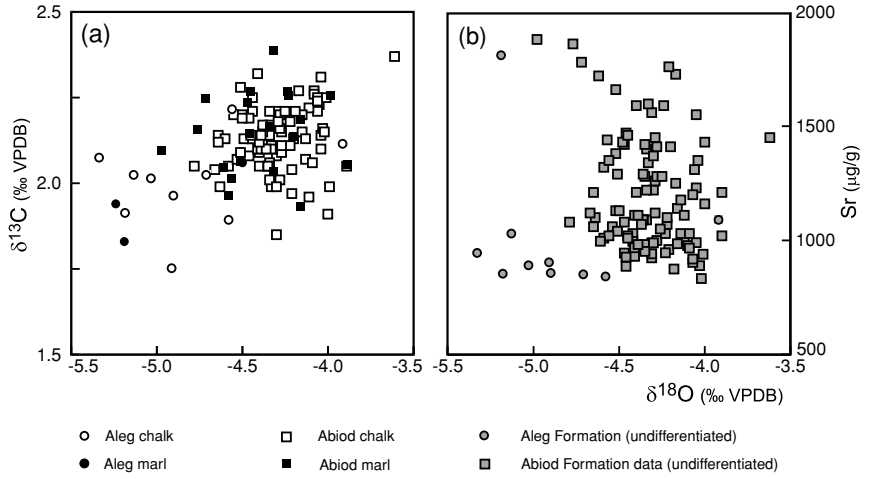

Fig. 6. Carbon isotope and strontium versus oxygen isotope crossplots for Miskar W1 samples. (a) Stable isotope crossplot; different symbols are used to differentiate between chalk and marl samples from the Aleg and Abiod formations. Note that samples with the lightest oxygen and carbon isotope values originate from the Aleg Formation; there is no separation between chalk and marl samples. (b) An oxygen isotope versus strontium crossplot indicates that the Aleg samples are generally depleted in Sr, $\delta^{13}C$, and $\delta^{18}O$, suggesting subaerial exposure of the uppermost Aleg Formation. However, burial diagenesis has induced lighter $\delta^{18}O$ values in both formations (mainly less than –3.5‰). Note that samples with Sr contents >2000 µg/g are excluded, as such high values are attributed to contamination by drilling mud.

Shackleton and Kennett (1975), we obtain average temperatures, in the Miskar W1 well, of 31.2°C and 34.4°C for the Abiod and the Aleg formations respectively and 35.3°C and 36.9°C for the two formations in the Miskar W4 well. The higher temperatures derived from the Miskar W4 samples confirm the burial diagenetic overprint in that well, but could the less altered chalks in Miskar W1 yield plausible palaeotemperatures?

Jenkyns *et al*. (1995), using data from bulk chalk samples buried to shallow depths in southern England, calculated maximum temperature of 27°C to 28°C for the English Chalk Sea at the Cenomanian-Turonian boundary, and documented falling temperatures through the Turonian - earliest Campanian. These values were, however, for an open-ocean influenced setting at a mid-palaeolatitude of around 40°N. At this time, Tunisia was situated much further south in the tropics at around 15°N, in the Northern Hot Arid Belt of Chumakov *et al*. (1995). The post-Turonian cooling at higher latitudes documented in the English Chalk may have been less significant in such tropical areas.

Clarke and Jenkyns (1999) extrapolated low-latitude maximum palaeotemperatures of 31–36°C for the Santonian, based on an isotope study of chalks in the southern hemisphere Exmouth Plateau. Glassy Turonian foraminifera preserved in clay-rich sediments from the tropics have yielded likely sea-surface palaeotemperatures of 28–32°C (Pearson *et al*., 2001; Wilson *et al*., 2002) at similar palaeolatitudes to Tunisia. General circulation models for the Cretaceous also yield high equatorial temperatures up to 34°C (Valdes *et al*., 1997).

The estimated palaeotemperature of 31.2°C derived from the least altered Abiod chalk samples in the Miskar W1 well lies, therefore, in the range of possible Late Cretaceous sea-surface temperatures for the southern Teythys Ocean, although the Aleg palaeotemperature of 34.4°C is probably too high. The substantially higher palaeotemperatures calculated from the other Miskar wells, however, demonstrate a significant burial diagenetic overprint in these despite only small differences of present-day burial depth. Offsets in the $\delta^{18}O$ values of different wells can be best ascribed to varying preservation controlled by different overpressuring and reservoir fill histories resulting from their varying positions on the Miskar structure. However, it is considered unlikely that the Miskar W1 well Abiod samples remain totally unaltered, but the degree of alteration is likely to be small. Below the basal unconformity, however, meteoric diagenesis has led to a significant negative shift in oxygen isotope values, generating unreliable high palaeotemperatures.

Conclusions

Our stable isotope study of the four Miskar wells has confirmed the probable unconformity between the Aleg and the Abiod Formation proposed by the biostratigraphic study of Bailey *et al*. (2000a, b). This has been illustrated through elemental and stable isotope crossplots and chemostratigraphic profiles which demonstrate that sig-

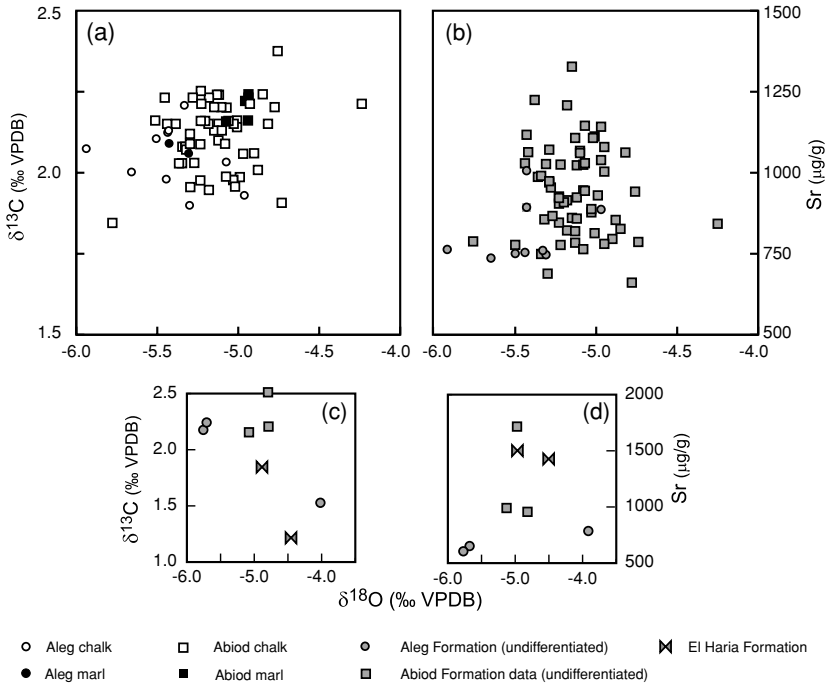

Fig. 7. Carbon isotope and strontium versus oxygen isotope crossplots for Miskar W2–W4 samples. (a, b) Miskar W4 data, (c, d) Miskar W2 and W3 data. Note that samples with the lightest oxygen isotope values and some of the lowest Sr contents in the Miskar W2 and W4 wells are from the Aleg Formation. Strontium and oxygen isotope depletion in the Aleg Formation is attributed to subaerial exposure at the unconformity between the Aleg and Abiod formations. Samples with Sr contents above 2000 µg/g are not plotted.

nificant depletion of Sr, $\delta^{13}C$ and $\delta^{18}O$ occurs in the uppermost Aleg Formation.

Variable burial diagenesis has affected the strontium and $\delta^{18}O$ contents of samples from all four Miskar wells, and can be assessed from offsets in their $\delta^{18}O$ values and curves. However, Abiod Formation samples from the Miskar W1 well demonstrate high $\delta^{18}O$ values that indicate reduced burial diagenesis caused by the early introduction of hydrocarbons and/or overpressuring. These samples yield plausible, if potentially unreliable, marine palaeotemperatures.

Carbon isotope values of the Abiod Formation in all of the Miskar wells, generally remain unaffected by burial diagenesis, and in most cases probably retain close to their original isotopic compositions. Carbon isotopes provide a means for inter-well correlation and might usefully be used for correlation with Campanian successions elsewhere. However, meteoric alteration of the top Aleg Formation during the Santonian has modified both the elemental and stable-isotope compositions of the Turonian-Coniacian section.

Acknowledgments—Research support by BG Exploration and Production and the British Council, Tunis (Chevening Scholarship TUN0100022 to Mabrouk) is gratefully acknowledged.

References

Abreu, V. S., Hardenbol, J., Haddad, G. A., Baum, G. R., Droxier, A. W. and Vail, P. R. (1998) Oxygen isotope synthesis: a Cretaceous ice-house? *Mesozoic and Cenozoic Sequence Stratigraphy of European Basins, Society of Economic Paleontologists and Mineralogists, Special Publication* (Graciansky, P.-C.d., Hardenbol, J., Jacquin, T. and Vail, P. R., eds.), **60**, 75–80.

Accarie, H., Emmanuel, L., Robaszynski, F., Amédro, F., Caron, M. and Deconnick, J. F. (1996) La géochimie isotopique du carbone ($\delta^{13}C$) comme outil stratigraphique. Application á la limite Cénomanien-Turonien en Tunisie centrale. *Comptes Rendus de l'Académie des Sciences, Paris* **322**, 579–586.

Anderson, T. F. and Arthur, M. A. (1983) Stable isotopes of oxygen and carbon and their application to sedimentologic and environmental problems. *Short Course, Society of Economic Paleontologists and Mineralogists* (Arthur, M. A., Anderson, T. F., Kaplan, I. R., Veizer, J. and Land, L. S., eds.), 1–151.

Apitz, S. E. (1991) The lithification of ridge flank basal carbonates: characterization and implications for Sr/Ca and Mg/Ca in marine chalks and limestones. Ph.D. Thesis, University of California, San Diego.

Arthur, M. A., Schlanger, S. O. and Jenkyns, U. C. (1987) The Cenomanian/Turonian Oceanic Anoxic Event, II: Palaeoceanographic controls on organic matter production and preservation. *Marine Petroleum Source Rocks. Special*

Publication of the Geological Society (Brooks, J. and Fleet, A. J., eds.), **26**, 401–420, London.

Arthur, M. A., Dean, W. E. and Pratt, L. M. (1988) Geochemical and climatic effects of increased marine organic carbon burial at the Cenomanian/Turonian boundary. *Nature*, **335**, 714–717.

Bailey, H. W., Hampton, M. J. and Gallagher, L. T. (2000a) Biostratigraphy of the Abiod limestone in wells Miskar-6, Miskar A-3, Miskar A7 and Miskar A11-ST2. BG E&P Internal Report, 29 pp.

Bailey, H. W., Hampton, M. J. and Gallagher, L. T. (2000b) Palaeoenvironmental interpretation of the Abiod limestone in wells Miskar-6, Miskar A-3, Miskar A7 and Miskar A11-ST2. BG E&P Internal Report, 9 pp.

British Gas (1990) Miskar Overview. BG E&P internal report.

Chumakov, N. M., Zharkov, M. A., Herman, A. B., Doludenko, M. P., Kalandadze, N. N., Lebedev, E. L., Ponomarenko, A. G. and Rautian, A. S. (1995) Climatic belts of the Mid-Cretaceous time. *Stratigraphy and Geological Correlation* **3**, 241–260.

Clarke, L. J. and Jenkyns, H. C. (1999) New oxygen isotope evidence for long-term Cretaceous climatic change in the Southern Hemisphere. *Geology* **27**, 699–702.

Craig, H. (1965) The measurement of oxygen isotope paleotemperatures. *Stable Isotopes in Oceanographic Studies and Paleotemperatures* (Tongiorgi, E., ed.), 161–182, Consiglio Nazionale delle Ricerche, Laboratorio di Geologica Nucleare, Pisa.

Douglas, C. and Savin, S. M. (1975) Oxygen isotopic evidence for the depth stratification of Tertiary and Cretaceous planktic foraminifera. *Marine Micropaleontology* **3**, 175–196.

Elorza, J., Garcia-Garmilla, F. and Jagt, J. W. M. (1997) Diagenesis-related differences and isotopic and elemental composition of Late Campanian and Early Maastrichtian inoceramids and belemnites from NE Belgium: Palaeoenvironmental implications. *Geologie en Mijnbouw* **75**, 349–360.

Emrich, K., Ehhalt, D. H. and Vogel, J.C . (1970) Carbon isotopes fractionation during the precipitation of calcium carbonate. *Earth Planet. Sci. Lett.* **8**, 363–371.

Epstein, S., Buchsbaum, R., Lowenstam, H. A. and Urey, H. C. (1953) Revised carbonate water isotopic temperature scale. *Geological Society of America Bulletin* **64**, 1315–1326.

Faure, G. (1986) *Principles of Isotope Geology*. Wiley, New-York, 147–151.

Gale, A. S., Jenkyns, H. C., Kennedy, W. J. and Corfield, R. M. (1993) Chemostratigraphy versus biostratigraphy: data from around the Cenomanian-Turonian boundary. *Jour. Geol. Soc. London* **150**, 29–32.

Gross, M. G. (1964) Variations in the $^{18}O/^{16}O$ and $^{13}C/^{12}C$ ratios of diagenetically altered limestones in the Bermuda islands. *J. Geol.* **72**, 172–193.

Grossman, E. L. and Ku, T. L. (1986) Oxygen and carbon isotope fractionation in biogenic aragonite: Temperature effects. *Chem. Geol.* **59**, 59–74.

Huber, B. T., Hodell, D. A. and Hamilton, C. P. (1995) Middle-Late Cretaceous climate of the southern high latitudes: Stable isotopic evidence for minimal equator-to-pole thermal gradients. *Geological Society of America Bulletin* **107**, 1164–1191.

Hudson, J. D. (1977) Stable isotopes and limestone lithification. *Jour. Geol. Soc. London* **133**, 637–660.

Jarvis, I. (1992) Sample preparation in ICP-MS. *Handbook of inductively Coupled Plasma Mass Spectrometry* (Jarvis, K. E., Gray, A. L. and Houk, R. S., eds.), 172–224, Blackie, Glasgow.

Jarvis, I. and Jarvis, K. E. (1992) Inductively coupled plasma-atomic emission spectrometry in exploration geochemistry. *Journal of Geochemical Exploration* **44**, 139–200.

Jarvis, I., Murphy, A. M. and Gale, A. S. (2001) Geochemistry of pelagic and hemipelagic carbonates: criteria for identifying Systems tracts and sea-level change. *Jour. Geol. Soc. London* **158**, 685–696.

Jarvis, I., Mabrouk, A., Moody, R. T. J. and de Cabrera, S. C. (2002) Late Cretaceous (Campanian) carbon isotope events, sea-level change and correlation of the Tethyan and Boreal realms. *Palaeogeogr. Palaeoclimatol. Palaeoecol.* **168**, 311–336.

Jenkyns, H. C. (1980) Cretaceous anoxic events: from continents to oceans. *Jour. Geol. Soc. London* **137**, 171–188.

Jenkyns, H. C. and Clayton, C. J. (1986) Black shales and carbon isotopes in pelagic sediments from the Tethyan Lower Jurassic. *Sedimentology* **33**, 87–106.

Jenkyns, H. C., Gale, A. S. and Corfield, R. M. (1994) Carbon- and oxygen-isotope stratigraphy of the English Chalk and Italian Scaglia and its palaeoclimatic significance. *Geological Magazine* **131**, 1–34.

Jenkyns, U. C., Multerlose, J. and Sliter, W. V. (1995) Upper Cretaceous carbon- and oxygen-isotope stratigraphy of deep-water sediments from the north-central Pacific (Site 869, flank of Pikinni Wodejebato, Marshall Islands). *Proceedings of the Ocean Drilling Project, Scientific Results* (Winterer, E. L., Sager, W. W., Firth, J. V. and Sinton, J. M., eds.), **143**, 105–108, College Station, TX (Ocean Drilling Program).

Jørgensen, N. O. (1981) Mg and Sr distribution in carbonate rocks from the Maastrichtian/Danian boundary of the Danish sub-basin and the North Sea Central Graben. *Sediment. Geol.* **30**, 311–325.

Jørgensen, N. O. (1986) Geochemistry, diagenesis and nannofacies of chalk in the North Sea Central Graben. *Sediment. Geol.* **48**, 267–294.

Jørgensen, N. O. (1987) Oxygen and carbon isotope composition of Upper Cretaceous Chalk from the Danish sub-basin and the North Sea Central Graben. *Sedimentology* **34**, 559–570.

Land, L. S. (1979) Chert-Chalk diagenesis, the Miocene island slope of north Jamaica. *Journal of Sedimentary Petrology* **49**, 223–232.

Land, L. S. (1986) Environments of limestone and dolomite diagenesis: some geochemical considerations. *Carbonate Depositional Environments. Modern and Ancient, Part 5, Diagenesis 1* (Bathurst, R. G. C. and Land, L. S., eds.), Quarterly of the Colorado School Mines, **81**, 26–41.

Land, L. S. and Epstein, S. (1970) Late Pleistocene diagenesis and dolomitization, North Jamaica. *Sedimentology* **14**, 187–200.

Li, L. Q., Keller, G., Adatte, T. and Stinnesbeck, W. (2000) Late Cretaceous sea-level changes in Tunisia: a multi-disciplinary approach. *Jour. Geol. Soc. London* **157**, 447–458.

Mabrouk, A. (2003) Chemostratigraphy and correlation of a chalk petroleum reservoir: the Upper Cretaceous Abiod Formation, Tunisia. Ph.D. Thesis, Kingston University, Kingston upon Thames, 476 pp.

Mabrouk, A., Jarvis, I., Belayouni, H., Moody, R. T. J. and de Cabrera, S. (2005) An integrated chemostratigraphic study of the Campanian-Early Maastrichtian deposits of the Offshore Miskar Field in southeastern Tunisia: SIS, $\delta^{13}C$ and $\delta^{18}O$ isotopes, and elemental geochemistry. *Stratigraphy* **2**(3), 193–216.

Malone, M. J., Baker, P. A., Burns, S. J. and Swart, P. K. (1990) Geochemistry of periplatform carbonate sediments, Leg 115, Site 716 (Maldives Archipelago, Indian Ocean). *Proceedings of the Ocean Drilling Program, Scientific Results* (Duncan, R. A., Backman, J., Peterson, L. C. *et al*., eds.), **115**, 647–659, College Station, TX (Ocean Drilling Program).

Marshall, J. D. (1981) Stable isotope evidence for the environment of lithification of some Tethyan limestones. *Neues Jahrbuch für Geologie und Paläontologie*, 211–224.

Marshall, J. D. (1992) Climatic and oceanographic isotopic signals from the carbonate rock record and their preservation. *Geol. Mag*. **129**, 143–160.

Matthews, A. and Katz, A. (1977) Oxygen isotope fractionation during dolomitization of calcium carbonate. *Geochim. Cosmochim. Acta* **41**, 1431–1438.

McCorkle, D. C., Martin, P. A., Lea, D. C. and Klinkhammer, G. P. (1995) Evidence of a dissolution effect on benthic foraminifera shell chemistry: $\delta^{13}C$, Cd/Ca, Ba/Ca, and Sr/Ca results from the Ontong Java Plateau. *Paleoceanography* **10**, 699–714.

Melim, L. A., Westphal, H., Swart, P. K., Eberli, G. P. and Munnecke, A. (2002) Questioning carbonate diagenetic paradigms: evidence from the Neogene of the Bahamas. *Marine Geol*. **185**, 27–53.

Mimran, Y. (1978) The induration of Upper Cretaceous Yorkshire and Irish Chalks. *Sediment. Geol*. **20**, 141–164.

Mitchell, S. F., Ball, J. D., Crowley, S. F., Marshall, J. D., Paul, C. R. C., Veltkamp, C. J. and Samir, A. (1997) Isotope data from Cretaceous chalk and foraminifera: Environmental or diagenetic signals? *Geology* **25**, 691–694.

Moody, R. T. J. and associates (1995) Core description, stratigraphy and sedimentology of Miskar A-11 (4851.00 m–4906.30 m), (5429.00 m–5400.10 m), Miskar offshore permit, Tunisia. BG E&P internal report.

Morse, J. W. and Mackenzie, F. T. (1990) *Geochemistry of Sedimentary Carbonates*. Developments in Sedimentology, 48, Elsevier, Amsterdam, 707 pp.

Negra, M. H. (1994) Les dépôts de plate-forme à bassin du Crétacé supérieur en Tunisie Centrale et Orientale (Formation Abiod et faciès associés). Stratigraphie, Sédimentation, Diagenèse et intérêt pétrolier. Thèse Doctorat es-Sciences, Université de Tunis, 649 pp.

Parrish, J. T. and Spicer, R. A. (1988) Middle Cretaceous wood from the Nanushuk Group, central North Slope, Alaska. *Palaeontology* **31**, 19–34.

Paul, C. R. C., Mitchell, S. F., Marshall, J. D., Leary, P. N., Gale, A. S., Duane, A. M. and Ditchfield, P. W. (1994) Palaeoceanographic events in the Middle Cenomanian of Northwest Europe. *Cret. Res*. **15**, 707–738.

Pearson, P. N., Ditchfield, P. W., Singano, J., Harcourt-Brown, K. G., Nicholas, C. J., Olsson, R. K., Shackleton, N. J. and Hall, M. A. (2001) Warm tropical sea surface temperatures in the Late Cretaceous and Eocene epochs. *Nature* **413**, 481–487.

Pomerol, B. (1983) Geochemistry of the late Cenomanian-early Turonian chalks of the Paris Basin: manganese and carbon isotopes in carbonates as palaeoceanographic indicators. *Cret. Res*. **4**, 85–93.

Renard, M. (1972) Interprétation des teneurs en strontium des carbonates du Lutétien supérieur à Saint Voart-Les-Mello (Oise). Mise en évidence de la valeur de cet élément comme indicateur des conditions de diagenèse et de sédimentation des carbonates. *Bulletin Information Géologique Bassin Paris* **34**, 19–29.

Renard, M. (1985) *Géochimie des Carbonates Pélagiques. Mis en Évidence des Fluctuations de la Composition des Eaux Océaniques depuis 140 Ma. Essai de Chimiostratigraphie*. Série de Documents du BRGM, 85, Éditions du Bureau de Recherches Géologiques et Minières, Orléans, 650 pp.

Renard, M. (1986) Pelagic carbonate chemostratigraphy (Sr, Mg, ^{18}O, ^{13}C). *Marine Micropalaeontology* **10**, 117–164.

Richter, F. M. and Turekian, K. K. (1993) Simple models for the geochemical response of the ocean to climatic and tectonic forcing. *Earth Planet. Sci. Lett*. **119**, 121–131.

Saint-Germes, M., Bocherens, H., Baudin, F. and Bazhenova, O. (2000) Evolution des valeurs de $\delta^{13}C$ des matières organiques de la série de Maykop au cours de l'Oligocène-Miocène inférieur. *Bulletin de la Société Géologique de France* **171**, 13–21.

Schlanger, S. O., Arthur, M. A., Jenkyns, H. C. and Scholle, P. A. (1987) The Cenomanian-Turonian Oceanic Event I. Stratigraphy and distribution of organic-carbon rich beds and the marine $\delta^{13}C$ excursion. *Marine Petroleum Source Rocks, Geological Society, London, Special Publication* (Brooks, J. and Fleet, A. J., eds.), **26**, 371–399.

ScholIe, P. A. (1974) Diagenesis of Upper Cretaceous chalks from England, Northern Ireland and the North Sea. *Pelagic Sediments on Land and under the Sea* (Hsu, K J. and Jenkyns, H J., eds.), International Association of Sedimentologists Special Publication, **1**, 177–210.

Scholle, P. A. (1977) Chalk diagenesis and its relation to petroleum exploration - oil from chalks, a modern miracle? *AAPG Bull*. **61**, 982–1009.

Scholle, P. A. and Arthur, M. A. (1980) Carbon isotope fluctuations in Cretaceous pelagic limestones: potential stratigraphic and petroleum exploration tool. *AAPG Bull*. **64**, 67–87.

Schönfeld, J., Sirocko, F. and Jørgensen, N. O. (1991) Oxygen isotope composition of Upper Cretaceous chalk at Lägerdorf (NW Germany): its original environmental signal and palaeotemperature interpretation. *Cret. Res*. **12**, 27–46.

Shackleton, N. J. and Kennett, J. P. (1975) Paleotemperature history of the Cenozoic and the initiation of Antarctic glaciation: oxygen and carbon isotope analyses in DSDP sites

277, 279, and 281 *Initial Reports of the Deep Sea Drilling Project* (Kennett, J. P., Houtz, R. E. *et al*., eds.), **29**, 743–755, US Government Printing Office, Washington, D.C.

Spicer, R. A. and Corfield, R. M. (1992) A review of terrestrial and marine climates in the Cretacous with implications for modelling the "Greenhouse Earth". *Geol. Mag*. **129**, 169–180.

Spicer, R. A. and Parrish, J. T. (1990) Late Cretaceous-Early Tertiary palaeoclimates of northern high latitudes: A quantitative view. *Jour. Geol. Soc. London* **147**, 329–341.

Stoll, H. M. and Schrag, D. P. (2001) Sr/Ca variations in Cretaceous carbonates: relation to productivity and sea level changes. *Palaeogeogr. Palaeoclimatol. Palaeoecol*. **168**, 311–336.

Tan, F. C. and Hudson, J. D. (1971) Carbon and oxygen isotopic relationships of dolomites and coexisting calcites, Great Estuarine Series (Jurassic) Scotland. *Geochim. Cosmochim. Acta* **35**, 755–767.

Tarutani, T., Clayton, R. N. and Mayeda T. K. (1969) The effect of polymorphism and magnesium substitution on oxygen isotope fractionation between calcium carbonate and water. *Geochim. Cosmochim. Acta* **33**, 987–996.

Totland, M., Jarvis, I. and Jarvis, K. E. (1992) An assessment of dissolution techniques for the analysis of geological samples by plasma spectrometry. *Chem. Geol*. **95**, 35–62.

Valdes, P. J., Sellwood, B. W. and Price, G. D. (1997) The concept of Cretaceous climate equability. *Palaeoclimates Data and Modelling* **1**, 139–158.

Weissert, H., Lini, A., Föllni, K. B. and Kuhn, O. (1998) Correlation of Early Cretaceous carbon isotope stratigraphy and platform drowning events: a possible link? *Palaeogeogr. Palaeoclimatol. Palaeoecol*. **137**, 189–203.

Wilson, P. A., Norris, R. D. and Cooper, M. J. (2002) Testing the Cretaceous greenhouse hypothesis using glassy foraminiferal calcite from the core of the Turonian tropics on Demerara Rise. *Geology* **30**, 607–610.

Zachos, J. C., Arthur, M. A. and Dean, W. E. (1989) Geochemical evidence for the suppression of pelagic marine productivity at the Cretaceous/Tertiary boundary. *Nature* **337**, 61–64.

Zachos, J. C., Scott, L. D. and Lohman, K. C. (1994) Evolution of Early Cenozoic marine temperatures. *Paleoceanography* **9**, 353–387.